AIMS Mathematics, 7(6): 11053–11069.
DOI: 10.3934/math.2022617
Received: 11 February 2022
Revised: 22 March 2022
Accepted: 23 March 2022
Published: 06 April 2022

http://www.aimspress.com/journal/Math

Research article

Calibration of time-dependent volatility for European options under the fractional Vasicek model

Jiajia Zhao and Zuoliang Xu*

School of Mathematics, Renmin University of China, Beijing 100872, China

* **Correspondence:** Email: xuzl@ruc.edu.cn.

Abstract: In this paper, we calibrate the time-dependent volatility function for European options under the fractional Vasicek interest rate model. A fully implicit finite difference method is applied to solve the partial differential equation of option pricing numerically. To find the volatility function, we minimize a cost function that is the sum of the squared errors between the theoretical prices and market prices with Tikhonov L_2 regularization and $L_{1/2}$ regularization respectively. Finally numerical experiments with simulated and real market data verify the efficiency of the proposed methods.

Keywords: calibration; fractional Vasicek model; European option; regularization; numerical methods
Mathematics Subject Classification: 65M32, 91G20, 90C32

1. Introduction

Black and Scholes [1] proved that option price satisfies a partial differential equation (PDE) under the strict assumptions and proposed the corresponding option pricing formula. However, the growing option market contradicts the assumptions in Black-Scholes model such as the logarithmic return distribution of underlying assets which usually shows the self similarity and long-term dependence in the real market [2–7]. A common method is to introduce another random term, such as stochastic interest rate or stochastic volatility, into the model of underlying price. Vasicek [8] derived a general form for the term structure of interest rates and gave the bond pricing formula in the form of a stochastic integral representation. Heston [28] assumed that the volatility follows a Cox-Ingersoll-Ross (CIR) process and deduced a closed-form pricing formula of European options. He and Chen [34] modified the Heston model with a stochastic mean-reversion level and gave a closed-form pricing formula based on the dimensional reduction technique. And there are many other researches under different stochastic volatility models [31–33].

Moreover, fractional Brownian motion (FBM) can describe the dynamics of underlying assets

which has long-term dependence. Mehrdoust and Najaf [9] obtained the explicit solution of fractional Black-Scholes model with weak payoff function. But Rogers [10] proved that it allows arbitrage opportunities. In order to solve this problem and consider the characteristics of long memory, Duncan et al. [11], Hu and Øksendal [12] developed a fractional white noise calculus and applied it to the market, which is modeled by Wick-Itô type of stochastic differential equations driven by fractional Brownian motion $B_H(t)(1/2 < H < 1)$. The corresponding Itô fractional Black-Scholes market has no arbitrage, and it is complete in contrast to the situation using the pathwise integration. Then Necula [13] obtained a fractional Black-Scholes formula for option price at $t \in [0, T]$ and a risk-neutral valuation theorem for the underlying which is driven by a fractional Brownian motion. Merton [14] gave the pricing formula of zero coupon bonds under the assumption that the corporate liabilities process obeys geometric Brownian motion and the interest rate changes randomly. Huang et al. [15] considered a model for complete and continuous market, and assumed that the process of asset price follows the geometric fractional Brownian motion and the interest rate process follows fractional Vasicek Interest rate model. The pricing formulas of European call option and put option were derived by using quasi martingale and partial differential equation method, and the parity formula was further obtained.

Volatility is a crucial parameter that affects option pricing, it is used to describe the price change of the underlying assets, and investors can use it to avoid some risks of assets price fluctuation in the future spot market. But it can not be directly observed in the market like the stock price. It is a considerable issue in finance to estimate volatility from the market price. Lagnado and Osher [18] put forward a technique for calibrating derivative security pricing models with respect to observed market prices, and estimated volatility from price observations by solving the inverse problem associated with the parabolic partial differential equation governing arbitrage-free derivative security prices. Chiarella et al. [19] suggested an improvement on the basis of Lagnado and Osher, avoiding the possibility of negative volatility, and gave the numerical algorithm of Euler-Lagrange equation. Jiang and Tao [20] applied an optimal control framework to determine implied volatility and made a rigorous mathematical analysis of this inverse problem. Ngnepieba [21] employed the unconstrained minimization algorithm of the quasi-Newton limited memory type to find the optimal volatility function, and computed the gradient via the adjoint method. He and Zhu [30] developed a two-step approach to calibrate the local volatility under the regime-switching models. Georgiev and Vulkov [22] presented a robust and fast numerical algorithm to reconstruct the implied volatility as a piecewise linear function of time. In this paper, we try to calibrate the time-dependent volatility of European options from a set of market observations under the fractional Vasicek model, using the Euler-Lagrange iterative method [16] and alternating direction method of multiplier (ADMM) [25], and give an empirical analysis of China's option market. Moreover, the proposed schemes also apply to the stochastic volatility models with mean reversion such as Heston model [28].

This paper is organized as follows: In Section 2, we present the the Vasicek fractional model for European option pricing and the corresponding inverse problem. In Section 3, we introduce the Tikhonov L_2 and $L_{1/2}$ regularization and analyse the stability of regularization model and the convergence of ADMM. The numerical verification is demonstrated in Section 4 with synthetic and real market data. Finally, some conclusions are stated in Section 5.

2. The mathematical formulation

In this section, we discuss the Vasicek fractional model for the European option. The dynamics of the model can be described as

$$\begin{aligned} dS &= rS\,dt + \sigma(t)S\,dB_H^1, \\ dr &= a(b-r)dt + \tau dB_H^2, \end{aligned} \tag{2.1}$$

where S is the underlying asset price, $\sigma(t)$ is the volatility, and r is the stochastic interest rate. a, b, τ are constants. H is the Hurst parameter, $B_H^j = \{B_H^j(t), t \geq 0, j = 1, 2\}$ are two correlated fractional Brown motion such that $Cov(dB_H^1, dB_H^2) = \rho(dt)^{2t}, (|\rho| < 1)$. Let $V(S, r, t)$ denote European option value under the model of (2.1), then $V(S, r, t)$ satisfies the following PDE [15]

$$\begin{aligned} \frac{\partial V}{\partial t} + H\sigma^2 S^2 t^{2H-1}\frac{\partial^2 V}{\partial S^2} + 2H\rho\sigma\tau S\, t^{2H-1}\frac{\partial^2 V}{\partial S\,\partial r} + H\tau^2 t^{2H-1}\frac{\partial^2 V}{\partial r^2} + rS\frac{\partial V}{\partial S} \\ + a\left(\tilde{b} - r\right)\frac{\partial V}{\partial r} - rV = 0, \end{aligned} \tag{2.2}$$

where $\tilde{b} = b - \frac{\lambda}{a}\tau$ and λ is the market price of risk.

Lemma 1. ***(European call option pricing formula)*** *Suppose that the underlying asset price S and interest rate r follow Vasicek fractional model* (2.1)*, then the price of a European call option with strike price K and maturity T can be expressed as*

$$V(S, r, t) = S\,N(\hat{d}_1) - KP(r, t; T)N(\hat{d}_2), \tag{2.3}$$

where $P(r, t; T)$ is the zero coupon bond

$$\begin{aligned} P(r, t; T) &= e^{-rB(t,T)-A(t,T)}, \quad B(t, T) = \frac{1}{a}(1 - e^{-a(T-t)}), \\ A(t, T) &= \widetilde{b}(T - t) - \widetilde{b}B(T - t) - H\int_t^T (\sigma^2(s)s^{2H-1}B^2(s, t))ds, \\ \hat{d}_1 &= \frac{\ln\frac{S}{K} - \ln P(r, t; T) + H\int_t^T \hat{\sigma}^2(s)s^{2H-1}ds}{\sqrt{2H\int_t^T \hat{\sigma}^2(s)s^{2H-1}ds}}, \\ \hat{d}_2 &= \hat{d}_1 - \sqrt{2H\int_t^T \hat{\sigma}^2(s)s^{2H-1}ds}, \\ \hat{\sigma}^2 &= \sigma^2 + 2\rho\sigma\tau B(t, T) + \tau^2 B^2(t, T), \end{aligned} \tag{2.4}$$

and $N(\cdot)$ denotes the standard normal cumulative distribution function.

In this paper, we only consider the European call option, the put option can be obtained by the put-call parity [15]. If the volatility $\sigma(t)$ is specified, the option price $V(S_0, r_0, 0, K, T, \sigma)$ can be uniquely determined by Lemma 1. Assume that the option prices $\{V_{ij}, i = 1, 2, ..., N, j = 1, 2, ..., M_i\}$ with maturities $\{T_i\}$ and the corresponding strike prices $\{K_{ij}\}$ are known, the inverse problem requires us to find a volatility function which makes the calibrated option value satisfy the following market quotes

$$V_{ij}^b \leq V(S_0, r_0, 0, K_{ij}, T_i, \sigma(t)) \leq V_{ij}^b, \tag{2.5}$$

where V_{ij}^b and V_{ij}^a represent the bid and ask price in market respectively.

Let $\mathcal{H}$ denote the measurable function space defined in $[0, T_{\max}]$, where $T_{\max}$ is the longest maturity. To satisfy (2.5), we use the available data to solve the following nonlinear problem.

Calibration problem: Given a series of market option prices $\{V_{ij}, i = 1, 2, ..., N, j = 1, 2, ..., M_i\}$, find a suitable volatility function $\sigma(t) \in \mathcal{H}$ to minimize the following error function

$$\Pi(\sigma) = \sum_{i=1}^{N} \sum_{j=1}^{M_i} [V(S_0, r_0, 0, K_{ij}, T_i, \sigma(t)) - V_{ij}]^2, \tag{2.6}$$

where $V_{ij} = (V_{ij}^a + V_{ij}^b)/2$, and the theoretical option value $V(S_0, r_0, 0, K_{ij}, T_i, \sigma(t))$ is obtained by Lemma 1.

However, there are not sufficient market observations to confirm the volatility $\sigma(t)$ uniquely, and the value of $\Pi(\sigma)$ is discontinuously dependent on the market data. Thus the calibration problem is ill-posed. In general, regularization is a practical technique to solve ill-posedness.

3. The regularization schemes for calibration problem

We employ two regularization schemes due to the ill-posedness of the volatility function minimizer. One is the Tikhonov L_2 regularization term $\|\sigma\|_2^2 + \|\nabla\sigma\|_2^2$, the other is $L_{1/2}$ regularization term $\|\sigma\|_{1/2}^{1/2} + \|\nabla\sigma\|_{1/2}^{1/2}$.

3.1. The Tikhonov L_2 regularization strategy

The Tikhonov L_2 regularization term we add is based on [16],

$$F_\alpha(\sigma) = \alpha \sum_{i=1}^{N} \sum_{j=1}^{M_i} [V(S_0, r_0, 0, K_{ij}, T_i, \sigma) - V_{ij}]^2 + \|\sigma\|_*^2, \tag{3.1}$$

where $\|\sigma\|_* := (\|\sigma\|_2^2 + \|\nabla\sigma\|_2^2)^{\frac{1}{2}}$, V_{ij} is a set of option prices in market and α is the regularization parameter. So we have

$$F_\alpha(\sigma) = \alpha \sum_{i=1}^{N} \sum_{j=1}^{M_i} [V(S_0, r_0, 0, K_{ij}, T_i, \sigma) - V_{ij}]^2 + \|\sigma\|_2^2 + \|\nabla\sigma\|_2^2. \tag{3.2}$$

Now, rewrite the right hand side of (3.2) as an integral

$$F_\alpha(\sigma) = \int_0^\infty \Big\{\alpha \sum_{i=1}^{N} \sum_{j=1}^{M_i} [V(t; S_0, r_0, K_{ij}, T_i, \sigma) - V_{ij}]^2 \delta(t) + \sigma^2(t) + (\sigma'(t))^2\Big\} dt, \tag{3.3}$$

where $\delta(t)$ is the Dirac delta function.

Suppose that

$$L(t, \sigma, \sigma') = \sigma^2(t) + (\sigma'(t))^2 + \alpha \sum_{i=1}^{N} \sum_{j=1}^{M_i} [V(t; S_0, r_0, K_{ij}, T_i, \sigma) - V_{ij}]^2 \delta(t). \tag{3.4}$$

We apply the Euler-Lagrange equations to $L(t, \sigma, \sigma')$ and obtain

$$\sigma'' - \sigma - \alpha \sum_{i=1}^{N} \sum_{j=1}^{M_i} \frac{\delta V}{\delta \sigma}(S_0, r_0, 0, K_{ij}, T_i, \sigma)[V(t; S_0, r_0, K_{ij}, T_i, \sigma) - V_{ij}] = 0, \tag{3.5}$$

with $\frac{\delta V_{ij}}{\delta \sigma} = \frac{\partial}{\partial \sigma} V(S_0, r_0, 0, K_{ij}, T_i, \sigma)\delta(t)$.

However, the above strategy calibrates volatility function at the fixed time $t_0 = 0$. Thus, the function $\sigma(t)$ derived from this method does not necessarily apply to future time. We can calibrate the volatility from the historical data [16], that is

$$H(\sigma) = \sum_{i=1}^{N} \sum_{j=1}^{M_i} \int_0^{T_{cur}} [V(t; S_0, r_0, K_{ij}, T_i, \sigma) - V_{ij}]^2 dt, \tag{3.6}$$

where T_{cur} is the current time.

Then apply L_2 regularization to minimize the following function

$$J_\alpha(\sigma) = \alpha H(\sigma) + \|\sigma\|_2^2 + \|\sigma'\|_2^2. \tag{3.7}$$

Now let us rewrite $J_\alpha(\sigma)$ as the integral form

$$J_\alpha(\sigma) = \int_0^{T_{cur}} \Big\{\alpha \sum_{i=1}^{N} \sum_{j=1}^{M_i} [V(t; S_0, r_0, K_{ij}, T_i, \sigma) - V_{ij}]^2 + \sigma^2(t) + (\sigma'(t))^2\Big\} dt. \tag{3.8}$$

Similarly, the Euler-Lagrange equation for (3.8) is

$$\sigma'' - \sigma - \alpha \sum_{i=1}^{N} \sum_{j=1}^{M_i} \frac{\partial V}{\partial \sigma}(t; S_0, r_0, K_{ij}, T_i, \sigma)[V(t; S_0, r_0, K_{ij}, T_i, \sigma) - V_{ij}] = 0, \tag{3.9}$$

with initial conditions $\sigma(t = 0)$ which can be determined from market data.

To solve Eq (3.9), we need to evaluate the term $\partial V(t; S_0, r_0, K_{ij}, T_i, \sigma)/\partial\sigma$. This variational derivative is defined for general arguments by

$$\frac{\partial V}{\partial \sigma}(t; S_0, r_0, K_{ij}, T_i, \sigma) = [\frac{d}{d\varepsilon} V(t; S_0, r_0, K_{ij}, T_i, \sigma + \varepsilon\delta)]_{\varepsilon=0}, \tag{3.10}$$

where the perturbation $\delta(t)$ is a Dirac delta function [18].

Such variational derivative can be calculated by solving a PDE (2.2) with an additional source term. Now consider the following partial differential operator

$$\begin{aligned} P_\sigma \;=\; & \frac{\partial}{\partial t} + H\sigma^2(t) S^2 t^{2H-1} \frac{\partial^2}{\partial S^2} + 2H\rho\sigma(t)\tau S t^{2H-1} \frac{\partial^2}{\partial S \partial r} + H\tau^2 t^{2H-1} \frac{\partial^2}{\partial r^2} + rS \frac{\partial}{\partial S} \\ & + a(\tilde{b} - r)\frac{\partial}{\partial r} - rI, \end{aligned} \tag{3.11}$$

where I denotes the identity operator.

The pricing function with a perturbed volatility satisfies a PDE similar to (2.2) of the form

$$P_{\sigma+\varepsilon\delta}V(t;S_0,r_0,K_{ij},T_i,\sigma+\varepsilon\delta)=0. \tag{3.12}$$

Then differentiate (3.12) with respect to ε and evaluate the value when $\varepsilon=0$, we have

$$\begin{aligned} P_\sigma\frac{\partial V}{\partial\sigma}(t;S_0,r_0,K_{ij},T_i,\sigma) &= -2HS^2\sigma(t)t^{2H-1}\frac{\partial^2 V}{\partial S^2}(t;S_0,r_0,K_{ij},T_i,\sigma) \\ &\quad -2H\rho\tau S\,t^{2H-1}\frac{\partial^2 V}{\partial S^2}(t;S_0,r_0,K_{ij},T_i,\sigma). \end{aligned} \tag{3.13}$$

The variational derivative satisfies homogeneous boundary and initial conditions [18], we can solve (3.13) for $\partial V/\partial\sigma$ numerically.

3.2. The $L_{1/2}$ regularization strategy

In this subsection, the $L_{1/2}$ regularization is considered, i.e., we calibrate volatility function by minimizing the following function

$$J_{\xi,\eta}(\sigma)=\frac{1}{2}\|V(\sigma)-\hat{V}\|^2+\xi\|\sigma\|_{1/2}^{1/2}+\eta\|\sigma'\|_{1/2}^{1/2}, \tag{3.14}$$

where $\|V(\sigma)-\hat{V}\|^2=\sum\limits_{i=1}^{N}\sum\limits_{j=1}^{M_i}[V(S_0,r_0,0,K_{ij},T_i,\sigma)-V_{ij}]^2$, $\|\sigma\|_{1/2}^{1/2}=\sum\limits_{i=1}^{N}|\sigma_i|^{1/2}$, $\sigma\in R^N$ and ξ,η are regularization parameters.

3.2.1. Numerical algorithm for $L_{1/2}$

To calibrate the time-dependent volatility $\sigma(t)$ from market data by $L_{1/2}$ regularization, we employ ADMM algorithm to obtain the convergent solution.

The augmented Lagrangian for the nonconvex optimization problem in (3.1) is

$$\min_{\sigma,y,z} l_\mu(\sigma,y,z):=\frac{1}{2}\|V(\sigma)-\hat{V}\|^2+\xi\|y\|_{1/2}^{1/2}+\eta\|z\|_{1/2}^{1/2}+\frac{\mu}{2}\|\sigma-y\|^2+\frac{\mu}{2}\|\nabla\sigma-z\|^2, \tag{3.15}$$

where $\mu>0$ is a regularization parameter.

Then we solve the augmented Lagrangian (3.15). Concretely, the procedure is as follows

$$\begin{cases} \sigma^{k+1}=\arg\min\limits_{\sigma} l_{\mu^k}(\sigma,y^k,z^k), \\ y^{k+1}=\arg\min\limits_{y} l_{\mu^k}(\sigma^{k+1},y,z^k), \\ z^{k+1}=\arg\min\limits_{z} l_{\mu^k}(\sigma^{k+1},y^{k+1},z), \\ \mu^{k+1}=\min\{\omega\mu^k,\overline{\mu}\}. \end{cases} \tag{3.16}$$

However, the algorithm (3.16) can not guarantee sufficient reduction for y_{k+1} and z_{k+1}. Based on [25], we have

$$\begin{cases} y^{k+1}=\arg\min\limits_{y}\Big\{l_{\mu^k}(\sigma^{k+1},y,z^k)+\frac{\delta\rho^k}{2}\|y-y^k\|^2\Big\}, \\ z^{k+1}=\arg\min\limits_{z}\Big\{l_{\mu^k}(\sigma^{k+1},y^{k+1},z)+\frac{\delta\rho^k}{2}\|z-z^k\|^2\Big\}. \end{cases} \tag{3.17}$$

For the σ sub-problems,

$$\sigma^{k+1} = \arg\min_{\sigma}\Big\{\frac{1}{2}\|V(\sigma^k) - \hat{V}\|^2 + \frac{\mu^k}{2}\|\sigma - y^k\|^2 + \frac{\mu^k}{2}\|\nabla\sigma - z^k\|^2\Big\}. \tag{3.18}$$

The corresponding Euler-Lagrange equation for (3.18) is

$$\sigma'' - \sigma = \frac{1}{\mu^k}\sum_{i=1}^{N}\sum_{j=1}^{M_i}[V(S_0, r_0, 0, K_{ij}, T_i, \sigma^k) - V_{ij}]\frac{\partial V}{\partial\sigma}(S_0, r_0, 0, K_{ij}, T_i, \sigma^k) - y^k + z'^k. \tag{3.19}$$

Since the sub-problems for y and z are nonconvex, nonsmooth and discontinuous, Xu et al. [24] proposed a reweighted iterative algorithm to solve this problem, which transforms $L_{1/2}$ regularization into L_1 term

$$y^{k+1} = \arg\min_{y}\Big\{\frac{\delta\rho^k + \mu^k}{2\xi}\|y - \frac{y^k\delta\rho^k + \sigma^k\mu^k}{\delta\rho^k + \mu^k}\|^2 + \sum_{i=1}^{N}\frac{|y_i|}{\sqrt{|y_i^k|} + \varepsilon}\Big\}, \tag{3.20}$$

where ε is a sufficient small constant to avoid the case $\sqrt{|y_i^k|} = 0$.

Then the following threshold iterative Algorithm 1 gives the local minimizer of y by applying accelerated approximate gradient method [27], where L denotes the Lipschitz constant.

Algorithm 1 Threshold iterative algorithm for fast solving $L_{1/2}$ problem

Require: $y^{-1} = y^0 = 0 \in R^N, t_{-1} = t_0 = 1, k = 0, \varepsilon > 0$.

Ensure: the optimization of (3.20)

1: **while** $\left\|y^{k+1} - y^k\right\|_2 < \varepsilon$ **and** $k < Maxiter$ **do**
2: $\quad\beta^{k+1} := y^k + \frac{t_{k+1}}{t_k}(y^k - y^{k-1})$,
3: $\quad g^{k+1} := \beta^{k+1} - \frac{\nabla f(\beta^{k+1})}{L} = \beta^{k+1} + \frac{2}{L}(\frac{y^k\delta\rho^k + \sigma^k\mu^k}{\delta\rho^k + \mu^k} - \beta^{k+1})$
4: $\quad$**if** $\left|g_i^{k+1}\right| > \frac{\sqrt[3]{54}}{4}(\frac{\lambda}{2L})^{\frac{2}{3}}$ **then**
5: $\quad\quad y_i^{k+1} = \frac{2}{3}g_i^{k+1}(1 + \cos(\frac{2\pi}{3} - \frac{2}{3}\arccos(\frac{\lambda}{4L}(\frac{|g_i^{k+1}|}{3})^{-\frac{2}{3}})))$
6: $\quad$**else**
7: $\quad\quad y_i^{k+1} = 0$
8: $\quad$**end if**
9: **end while**
10: **return** *result*

As for the sub-problem of z,

$$z^{k+1} = \arg\min_{z}\Big\{\|z\|_{1/2}^{1/2} + \frac{\delta\rho^k + \mu^k}{2\eta}\|z - \frac{z^k\delta\rho^k + \mu^k\nabla\sigma^k}{\delta\rho^k + \mu^k}\|^2\Big\}. \tag{3.21}$$

Similarly, the minimizer of z can be obtained by the analogical process as Algorithm 1.

3.2.2. Convergence analysis

Now we discuss the convergence of the above algorithm [25,26].

Theorem 3.1. *Let* $\{(\sigma^k, y^k, z^k)\}$ *be the sequence generated by ADMM algorithm, then*

1) $\{(\sigma^k, y^k, z^k)\}$ *is a minimization sequence, and* $l_{\overline{\mu}}(\sigma^k, y^k, z^k)$ *converges to* $l_{\overline{\mu}}(\sigma^*, y^*, z^*)$*, where* (σ^*, y^*, z^*) *is a limit point of minimization sequence* $\{(\sigma^k, y^k, z^k)\}$*;*

2) $\{(\sigma^k, y^k, z^k)\}$ *is asymptotically regular, i.e.,* $\lim\limits_{n\to\infty} \|\sigma^{k+1} - \sigma^k\| = \lim\limits_{n\to\infty} \|y^{k+1} - y^k\| = \lim\limits_{n\to\infty} \|z^{k+1} - z^k\| = 0$*;*

3) $\{(\sigma^k, y^k, z^k)\}$ *converges to the stationary point of* $l_{\overline{\mu}}(\sigma, y, z)$*.*

Proof. 1) Let $k > \ln \frac{\bar{\mu}}{\mu_0} \Big/ \ln \omega + 1$, then $\mu^k = \overline{\mu}$. Since $l_{\overline{\mu}}(\sigma, y^k, z^k)$ is strongly convergent for σ, and $\sigma^{k+1} \in \arg\min\limits_{\sigma} l_{\overline{\mu}}(\sigma, y^k, z^k)$, then

$$l_{\overline{\mu}}(\sigma^k, y^k, z^k) - l_{\overline{\mu}}(\sigma^{k+1}, y^k, z^k) \geq \frac{\overline{\mu}}{2}\|\sigma^{k+1} - \sigma^k\|^2. \tag{3.22}$$

Similarly, the following inequalities hold

$$l_{\overline{\mu}}(\sigma^{k+1}, y^k, z^k) \geq l_{\overline{\mu}}(\sigma^{k+1}, y^{k+1}, z^k) + \frac{\delta\overline{\mu}}{2}\|y^{k+1} - y^k\|^2, \tag{3.23}$$

$$l_{\overline{\mu}}(\sigma^{k+1}, y^{k+1}, z^k) \geq l_{\overline{\mu}}(\sigma^{k+1}, y^{k+1}, z^{k+1}) + \frac{\delta\overline{\mu}}{2}\|z^{k+1} - z^k\|^2. \tag{3.24}$$

Combine (3.22)–(3.24), we can obtain

$$\begin{aligned} l_{\overline{\mu}}(\sigma^k, y^k, z^k) - l_{\overline{\mu}}(\sigma^{k+1}, y^{k+1}, z^{k+1}) \quad \geq \quad & \frac{\overline{\mu}}{2}\|\sigma^{k+1} - \sigma^k\|^2 + \frac{\delta\overline{\mu}}{2}\|y^{k+1} - y^k\|^2 \\ & + \frac{\delta\overline{\mu}}{2}\|z^{k+1} - z^k\|^2. \end{aligned} \tag{3.25}$$

That is, $\{(\sigma^k, y^k, z^k)\}$ is a minimization sequence of $l_{\overline{\mu}}(\sigma, y, z)$, and $l_{\overline{\mu}}(\sigma^k, y^k, z^k)$ is monotonically decreasing to a fixed value l^*.

Since $(\sigma^k, y^k, z^k) \in B = \{(\sigma, y, z) : l_{\overline{\mu}}(\sigma, y, z) \leq l_{\overline{\mu}}(\sigma^0, y^0, z^0)\}$, which is bounded, $\{(\sigma^k, y^k, z^k)\}$ is bounded and has a limit point (σ^*, y^*, z^*). By continuity of $l_{\bar{\mu}}(\sigma, y, z)$ and monotonicity of $l_{\overline{\mu}}(\sigma^k, y^k, z^k)$, we have $l^* = l_{\overline{\mu}}(\sigma^*, y^*, z^*)$.

2) Note that $l_{\overline{\mu}}(\sigma, y, z) \geq 0$, and there is a sufficiently large K such that

$$\begin{aligned} \sum_{j=K}^{k} \Big\{ \frac{\overline{\mu}}{2}\|\sigma^{j+1} - \sigma^j\|^2 + \frac{\delta\overline{\mu}}{2}\|y^{j+1} - y^j\|^2 + \frac{\delta\overline{\mu}}{2}\|z^{j+1} - z^j\|^2 \Big\} \\ \leq l_{\overline{\mu}}(\sigma^K, y^K, z^K) - l_{\overline{\mu}}(\sigma^{k+1}, y^{k+1}, z^{k+1}) < \infty. \end{aligned} \tag{3.26}$$

Let $k \to \infty$, we can conclude that

$$\lim_{k\to\infty} \|\sigma^{k+1} - \sigma^k\| = \lim_{k\to\infty} \|y^{k+1} - y^k\| = \lim_{k\to\infty} \|z^{k+1} - z^k\| = 0. \tag{3.27}$$

3) By 1) and 2), the sequence $\{(\sigma^k, y^k, z^k)\}$ is asymptotically regular and $\lim_{k\to\infty} l_{\bar{\mu}}(\sigma^k, y^k, z^k) = l_{\bar{\mu}}(\sigma^*, y^*, z^*)$. We further show that (σ^*, y^*, z^*) is a stationary point of $l_{\bar{\mu}}(\sigma^k, y^k, z^k)$.

Since σ^{k+1} is the minimizer of $l_{\bar{\mu}}(\sigma, y^k, z^k)$, it implies $\partial_\sigma l_{\bar{\mu}}(\sigma^{k+1}, y^k, z^k) = 0$. Similarly,

$$\begin{aligned} &\partial_y l_{\bar{\mu}}(\sigma^{k+1}, y^{k+1}, z^k) + \delta\mu(y^{k+1} - y^k) = 0, \\ &\partial_z l_{\bar{\mu}}(\sigma^{k+1}, y^{k+1}, z^{k+1}) + \delta\mu(z^{k+1} - z^k) = 0. \end{aligned} \tag{3.28}$$

Let $k \to \infty$, this yields

$$\begin{aligned} &\partial_\sigma l_{\bar{\mu}}(\sigma^*, y^*, z^*) = 0, \\ &\partial_y l_{\bar{\mu}}(\sigma^*, y^*, z^*) = 0, \\ &\partial_z l_{\bar{\mu}}(\sigma^*, y^*, z^*) = 0. \end{aligned} \tag{3.29}$$

That is, (σ^*, y^*, z^*) is the stationary point of $l_{\bar{\mu}}(\sigma, y, z)$. □

4. Computational experiments

In this section, we use numerical simulation and empirical analysis to verify the effectiveness of the proposed methods.

4.1. Numerical simulation

Here we consider the following synthetic volatility function

$$\sigma(t) = 0.2 - 0.1 \ln(1.5 + 3t). \tag{4.1}$$

Let $K = \{64, 68, 72, 76, 80\}, T = \{0.5, 1\}$, then $S_{\max} = 2K_{\max} = 160$, and $r_{\max} = 0.25$, the initial value $S_0 = 62, r_0 = 0.025, \sigma_0 = 0.15$, the parameters values involved in the interest rate model are $a = 0.2, b = 0.05, \tau = 0.3, \rho = 0.4, \lambda = 0.2$. According to the calibration results and [25], we get the parameters in L_2 and $L_{1/2}$ regularization in Table 1.

Table 2 compares the reconstructed and real volatility when the Hurst index $H = 0.5, 0.6, 0.7, 0.8, 0.9$ under L_2 and $L_{1/2}$ regularization. A common measure $RMSE$ is used to evaluate the accuracy of reconstructed volatility $\sigma(t)$ compared with exact volatility $\hat{\sigma}(t)$, and it is defined as

$$RMSE = \sqrt{\frac{1}{n}\sum_{i=1}^{n} |\sigma_i - \hat{\sigma}_i|^2}.$$

The European call option prices generated by Lemma 1 and volatility function (4.1) are represented in Table 3. Figure 1 and Figure 2 show the calibration results. We can see that both schemes can satisfactorily recover the exact volatility function, and $L_{1/2}$ regularization is slightly more accurate than L_2 regularization. The results indicate that there is a long-term correlation from the volatility itself long term correlation when Hurst index is higher than 0.5, and it is consistent with the existing research on the recurrence interval in finance [8].

Table 1. Parameters of L_2 and $L_{1/2}$ regularization.

L_2 Regularization	$L_{1/2}$ Regularization
$\alpha = 0.004$	$\xi = 0.2, \eta = 0.1, \mu = 1, \omega = 3, \bar{\mu} = 10^8, L = 3.5$

Table 2. The numerical results of different Hurst index.

H	L_2 Regularization		$L_{1/2}$ Regularization	
	$RMSE$	$\max\|\sigma - \hat{\sigma}\|$	$RMSE$	$\max\|\sigma - \hat{\sigma}\|$
0.5	7.5784e-4	1.0734e-3	6.2822e-4	9.5349e-4
0.6	6.8186e-4	1.1832e-3	2.5348e-4	9.5349e-4
0.7	6.7642e-4	1.3055e-3	2.5377e-4	9.5349e-4
0.8	7.2259e-4	1.4207e-3	4.9045e-4	9.5349e-4
0.9	7.9211e-4	1.5240e-3	7.1061e-4	1.0423e-3

Table 3. The numerical results of different Hurst index.

K	62	66	70	74	78
$T_1 = 180/360$	2.2468	1.0648	0.4491	0.1701	0.0585
$T_2 = 360/360$	4.9177	3.5529	2.5226	1.7638	1.2167

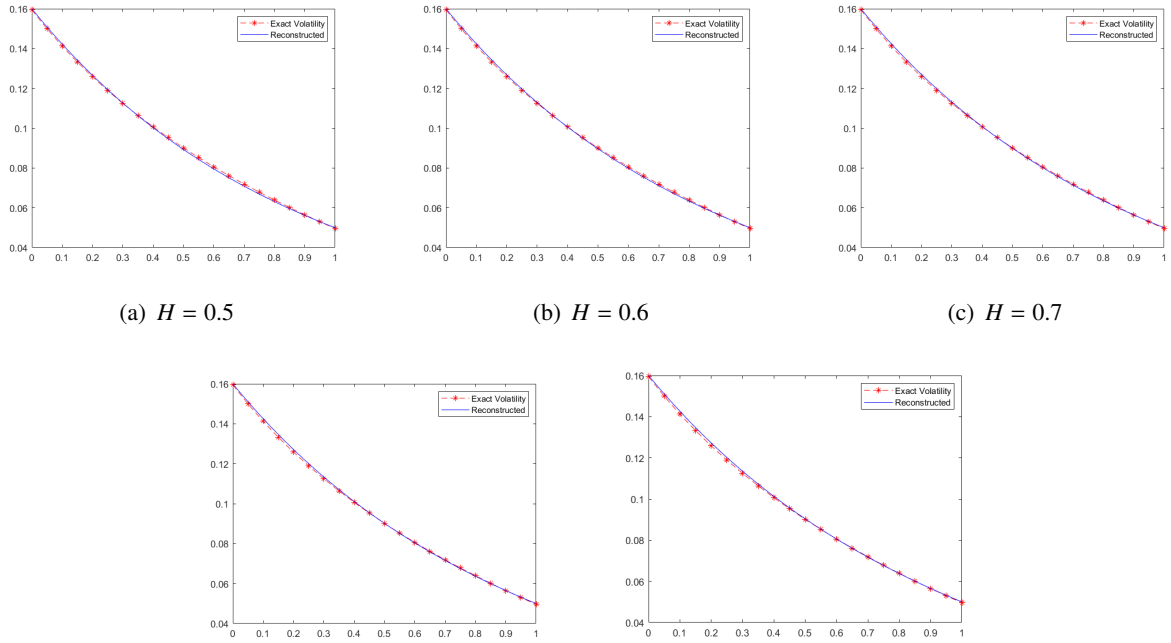

(a) $H = 0.5$ (b) $H = 0.6$ (c) $H = 0.7$

(d) $H = 0.8$ (e) $H = 0.9$

Figure 1. The calibration results by L_2 regularization.

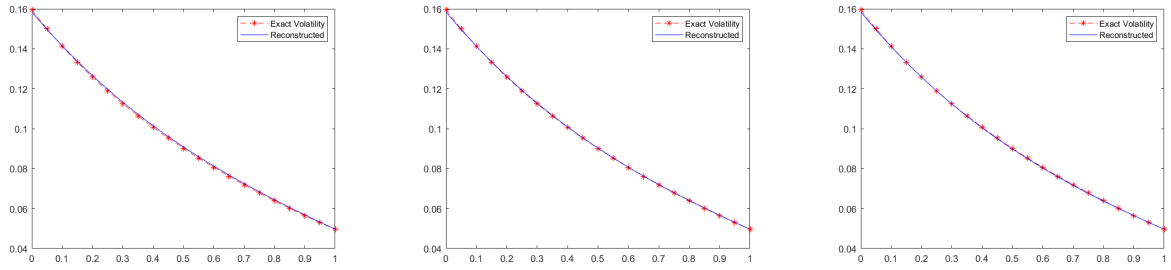

(a) $H = 0.5$ (b) $H = 0.6$ (c) $H = 0.7$

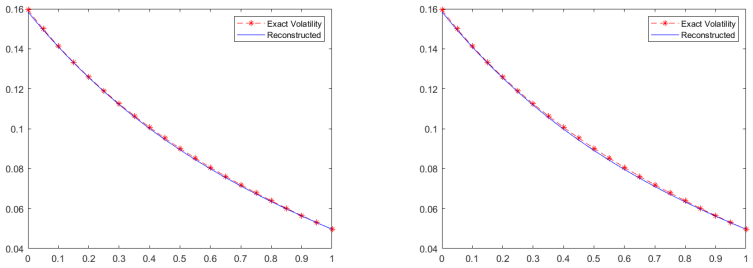

(d) $H = 0.8$ (e) $H = 0.9$

Figure 2. The calibration results by $L_{1/2}$ regularization.

4.2. Stability test

To emphasize the stability of both methods, we introduce a random variable x which follows the standard normal distribution [29,30], and the volatility function with noise is

$$\sigma(t) = [0.2 - 0.1\ln(1.5 + 3t)](1 + 0.2x).$$

Using the noised volatility, we can obtain the corresponding noised option prices in market, which will be employed to reconstruct volatility function with the proposed algorithms. The iteration stop criterion is $max\,|\sigma_d(t) - \sigma_{d-1}(t)| < 10^{-7}$ and the maximum number of iterations is 200, where $\sigma_d(t)$ is the volatility function reconstructed in the dth iteration. Figure 3 compares the reconstructed and real volatility under L_2 and $L_{1/2}$ schemes when Hurst parameter is $H = 0.7$. Table 4 gives the comparison of stability results between L_2 and $L_{1/2}$ schemes. We can conclude that the performance of Hurst index H in the range of 0.6 to 0.8 is better than that of standard Brownian motion with $H = 0.5$, and $L_{1/2}$ regularization has slightly smaller deviation than L_2 scheme. And both methods are stable since the recovered time-dependent volatility resembles the exact function though adding a little disturbance.

Table 4. The numerical results of stability test.

Scheme	L_2	$L_{1/2}$
$\max\|\sigma - \hat{\sigma}\|$	8.3669e-3	7.3734e-3
$RMSE$	4.4719e-3	3.5987e-3

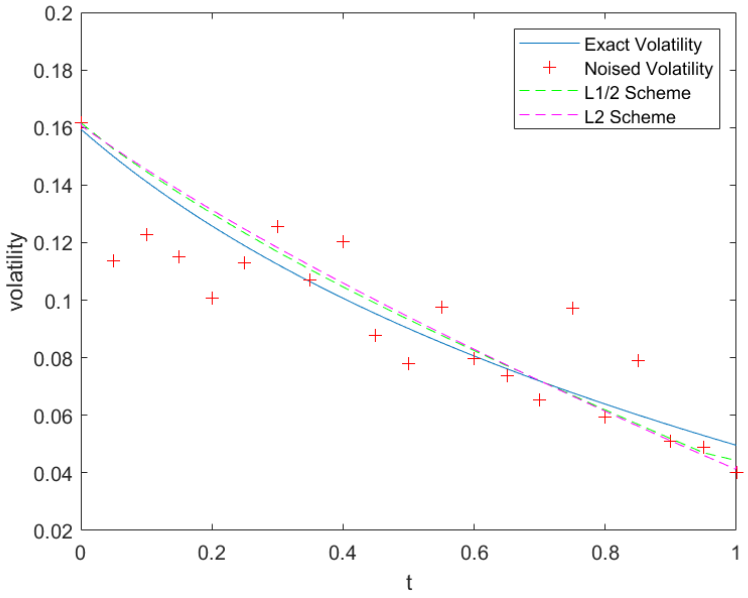

Figure 3. The calibration results by noised data.

4.3. Empirical analysis

Now we calibrate the volatility from the price of Shanghai Stock Exchange(SSE) 50ETF on 9th September, 2021, which are shown in Table 5. The data set is provided by Wind Info, Inc. The current value of the SSE 50ETF was $S_0 = 3.204$. The SSE 50 ETF options have four types of expiration months: The current month, the next month, and the first month of the following two consecutive quarters, so the days to expiration are $T_1 = 13, T_2 = 48, T_3 = 104, T_4 = 195$. We choose Shanghai Inter Bank Offered Rate (SHIBOR) 1M at 9th September as initial interest rate $r_0 = 2.323\%$ and historical volatility as $\sigma_0 = 0.2161$.

In order to measure the quality of the calibrated volatility by different Hurst parameters, we use root mean squared error (RMSE) between the recalculated option price by model and market price. The accuracy of calibrated volatility has reported in Table 6 and Figures 4–6. The results indicate that $H = 0.6$ has a much smaller RMSE than $H = 0.5$ and performs better for far-month options.

It is clear that the fractional model such as $H = 0.6$ performs better than the general geometric Brownian model where $H = 0.5$ due to the long-term dependence of fractional Brownian motion. In China's stock market dominated by individual investors, the high-frequency and short-term trading behavior is relatively common, which results in the short-term and medium-term factors occupying the dominant position in the market [35]. Thus the predicted price corresponding to the longest maturity $T = T_4$ significantly differ from the actual market price, and we can see that the predicted price of far-month option is higher than the actual price for European call option. In addition, for short-term contracts of the current month $T = T_1$, the pricing error of out-of-the-money option is higher than the in-the-money, which is mainly caused by extrapolation and fitting [36].

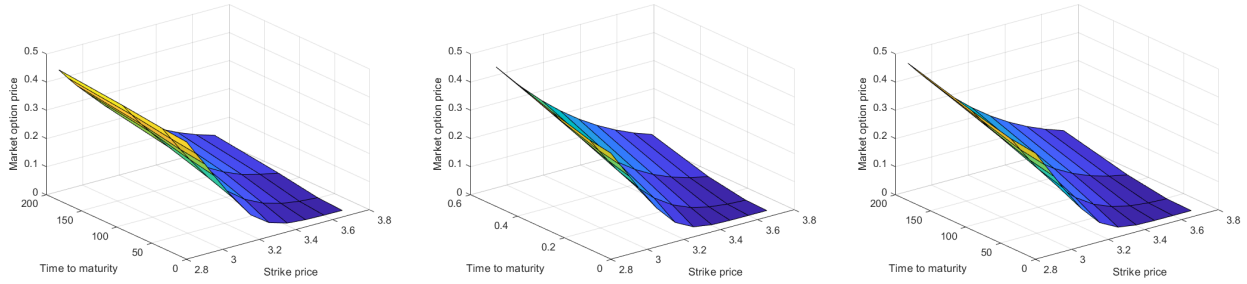

Figure 4. Left: market price; middle: L_2 scheme; right: $L_{1/2}$ scheme.

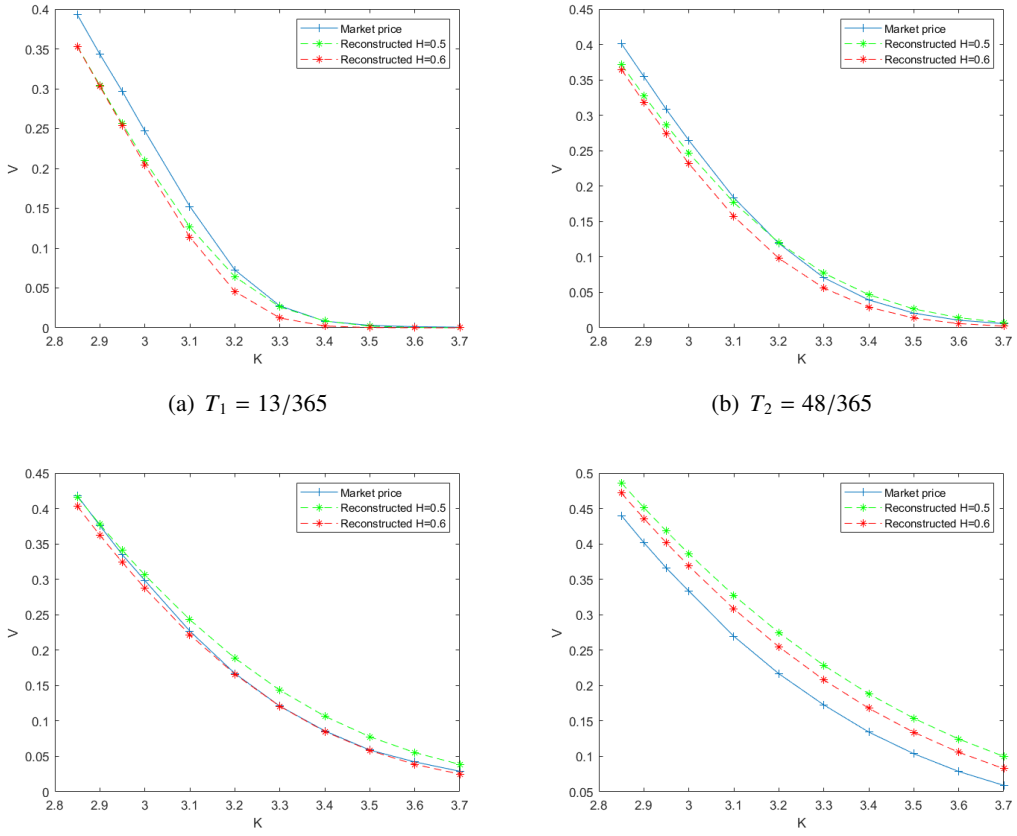

(a) $T_1 = 13/365$ (b) $T_2 = 48/365$

(c) $T_3 = 104/365$ (d) $T_4 = 195/365$

Figure 5. Comparison of SSE 50ETF price with numerical prices with $H = 0.6$ by L_2 scheme.

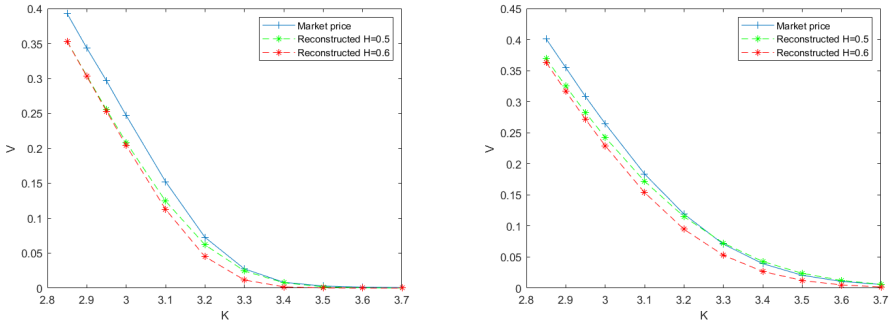

(a) $T_1 = 13/365$ (b) $T_2 = 48/365$

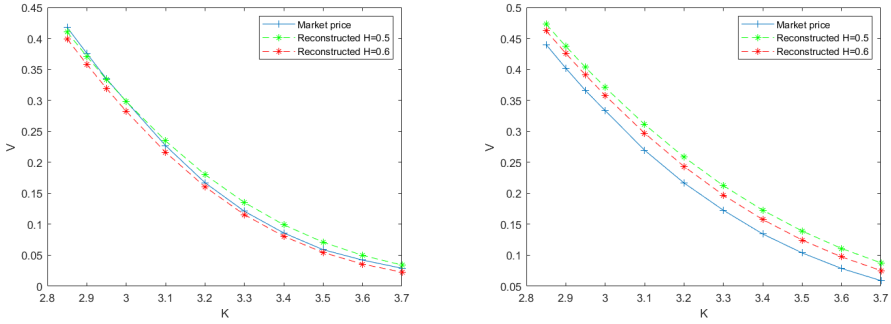

(c) $T_3 = 104/365$ (d) $T_4 = 195/365$

Figure 6. Comparison of SSE 50ETF price with numerical prices with $H = 0.6$ by $L_{1/2}$ scheme.

Table 5. The SSE 50ETF option price at 9th September, 2021.

Strike Price K	$V(K, T_1)$	$V(K, T_2)$	$V(K, T_3)$	$V(K, T_4)$
2.85	0.3928	0.4013	0.4179	0.4401
2.90	0.3434	0.3548	0.3758	0.4019
2.95	0.2966	0.3082	0.3347	0.3659
3.00	0.2470	0.2647	0.2984	0.3334
3.10	0.1523	0.1837	0.2269	0.2695
3.20	0.0726	0.1192	0.1671	0.2167
3.30	0.0275	0.0707	0.1210	0.1727
3.40	0.0084	0.0393	0.0860	0.1343
3.50	0.0030	0.0207	0.0590	0.1038
3.60	0.0014	0.0107	0.0422	0.0787
3.70	0.0008	0.0059	0.0290	0.0591

Table 6. The numerical results of different Hurst index.

Hurst Index H		0.5	0.6	0.7	0.8	0.9
L_2	iterations	4	4	5	4	4
	$\max \lvert\sigma_d - \sigma_{d-1}\rvert$	3.0631e-10	7.6086e-9	6.3632e-11	2.8506e-09	5.7676e-09
	V $RMSE$	0.0309	0.0258	0.0269	0.0313	0.0364
	$\max \left\lvert V - \hat{V}\right\rvert$	0.0589	0.0431	0.0451	0.0541	0.0668
$L_{1/2}$	iterations	29	29	29	29	29
	$\max \lvert\sigma_d - \sigma_{d-1}\rvert$	7.4981e-5	7.4868e-5	7.4798e-5	7.4755e-5	7.4738e-5
	V $RMSE$	0.0248	0.0239	0.0270	0.0314	0.0359
	$\max \left\lvert V - \hat{V}\right\rvert$	0.0428	0.0434	0.0459	0.0543	0.0652

5. Conclusions

In this paper, we consider the Tikhonov L_2 and $L_{1/2}$ regularization for the construction of a time-dependent volatility function from a finite set of market observations by the fractional Vasicek model. A fully implicit finite difference method is applied to solve the direct problem numerically. Several examples are given to demonstrate the accuracy and robustness of our proposed algorithms. The calibration results indicate that the Hurst index H ranging from 0.6 to 0.8 performs better than $H = 0.5$, and $L_{1/2}$ regularization has slightly smaller deviation but longer running time than L_2 scheme.

Acknowledgments

The work was supported by the National Natural Science Foundation of China (Grant No. 12071479). The authors would like to thank the referees for the helpful suggestions.

Conflict of interest

The authors declare no conflict of interest in this paper.

References

1. F. Black, M. Scholes, The pricing of option and corporate liabilities, *J. Polit. Econ.*, **81** (1973), 637–654. https://doi.org/10.1086/260062
2. W. G. Zhang, Z. Li, Y. J. Liu, Y. Zhang, Pricing European option under fuzzy mixed fractional Brownian motion model with jumps, *Comput. Econ.*, **58** (2021), 483–515. https://doi.org/10.1007/s10614-020-10043-z
3. A. W. Lo, Long-term memory in stock market prices, *Econometrica*, **59** (1991), 1279–313. https://doi.org/10.2307/2938368
4. S. Sadique, P. Silvapulle, Long-term memory in stock market returns: International evidence, *Int. J. Financ. Econ.*, **6** (2001), 59–67. https://doi.org/10.1002/ijfe.143

5. A. Sensoy, B. M. Tabak, Time-varying long term memory in the European Union stock markets, *Physica A*, **436** (2015), 147–158. https://doi.org/10.1016/j.physa.2015.05.034
6. A. Sensoy, B. M. Tabak, Dynamic effciency of stock markets and exchange rates, *Int. Rev. Financial Anal.*, **47** (2016), 353–371. https://doi.org/10.1016/j.irfa.2016.06.001
7. J. T. Barkoulas, A. G. Barilla, W. Wells, Long-memory exchange rate dynamics in the euroera, *Chaos Soliton. Fract.*, **86** (2016), 92–100. https://doi.org/10.1016/j.chaos.2016.02.007
8. O. A. Vasicek, An equilibrium characterization of the term structure, *J. Financ. Econ.*, **5** (1977), 177–188. https://doi.org/10.1016/0304-405X(77)90016-2
9. F. Mehrdoust, A. R. Najaf, Pricing European options under fractional Black-Scholes model with a weak payoff function, *Comput. Econ.*, **52** (2018), 685–706. https://doi.org/10.1007/s10614-017-9715-3
10. L. C. G. Rogers, Arbitrage with fractional Brownian motion, *Math. Financ.*, **7** (1997), 95–105. https://doi.org/10.1111/1467-9965.00025
11. T. E. Duncan, Y. Hu, B. Pasik-Duncan, Stochastic calculus for fractional Brownian motion, *SIAM J. Control. Optim.*, **38** (2000), 582–612. https://doi.org/10.1137/S036301299834171X
12. Y. Hu, B. Øksendal, Fractional white noise calculus and applications to finance, *Infin. Dimens. Anal. Qu.*, **6** (2003), 1–32. https://doi.org/10.1142/S0219025703001110
13. C. Necula, Option pricing in a fractional brownian motion environment, *Math. Rep.*, **6** (2004), 259–273. https://dx.doi.org/10.2139/ssrn.1286833
14. R. C. Merton, On the pricing of corporate debt: The risk structure of interest rates, *J. Financ.*, **29** (1974), 449–470. https://doi.org/10.1111/j.1540-6261.1974.tb03058.x
15. W. L. Huang, X. X. Tao, S. H. Li, Pricing formulae for European options under the fractional Vasicek interest rate model, *Acta Math. Sin.*, **55** (2012), 219–230.
16. Z. L. Xu, X. Y. Jia, The calibration of volatility for option pricing models with jump diffusion processes, *Appl. Anal.*, **98** (2019), 810–827. https://doi.org/10.1080/00036811.2017.1403588
17. A. Kirsch, *An introduction to the mathematical theory of inverse problems*, Springer, 2011.
18. R. Lagnado, S. Osher, A technique for calibrating derivative security pricing models: Numerical solution of an inverse problem, *J. Comput. Financ.*, **1** (1997), 13–25. https://doi.org/10.21314/JCF.1997.002
19. C. Chiarella, M. Craddock, N. El-Hassan, The calibration of stock option pricing models using inverse problem methodology, *QFRQ Res. Paper Ser.*, 2000.
20. L. S. Jiang, Y. S. Tao, Identifying the volatility of underlying assets from option prices, *Inverse Probl.*, **17** (2001), 137–155. https://doi.org/10.1088/0266-5611/17/1/311
21. P. Ngnepieba, The adjoint method formulation for an inverse problem in the generalized Black-Scholes model, *J. Syst. Cybern. Inform.*, **4** (2006), 69–77.
22. S. G. Georgiev, L. G. Vulkov, Fast reconstruction of time-dependent market volatility for European options, *Comput. Appl. Math.*, **40** (2021), 30–48. https://doi.org/10.1007/s40314-021-01422-9
23. R. Ramlau, C. A. Zarzer, On the minimization of a Tikhonov functional with a non-convex sparsity constraint, *Electron. Trans. Numer. Anal.*, **39** (2012), 476–507.

24. Z. B. Xu, X. Y. Chang, H. Zhang, Y. Wang, $L_{1/2}$ *regularization*, Science China, 2010.

25. T. Sun, D. S. Li, Nonconvex low-rank and total-variation regularized model and algorithm for image deblurring, *Chinese J. Comput.*, **43** (2020), 643–652.

26. Z. B. Xu, X. Y. Chang, F. M. Xu, H. Zhang, $L_{1/2}$ Regularization: A thresholding representation theory and a fast solver, *IEEE T. Neur. Net. Lear.*, **23** (2012), 1013–1027. https://doi.org/10.1109/TNNLS.2012.2197412

27. A. Beck, M. Teboulle, A fast iterative shrinkage-thresholding algorithm for linear inverse problems, *SIAM J. Imaging Sci.*, **2** (2009), 183–202. https://doi.org/10.1137/080716542

28. S. L. Heston, A closed-form solution for options with stochastic volatility with applications to bond and currency options, *Rev. Financ. Stud.*, **6** (1993), 327–343. https://doi.org/10.1093/rfs/6.2.327

29. X. J. He, S. P. Zhu, How should a local regime-switching model be calibrated? *J. Econ. Dyn. Control.*, **78** (2017), 149–163. https://doi.org/10.1016/j.jedc.2017.03.005

30. X. J. He, S. P. Zhu, On full calibration of hybrid local volatility and regime-switching models, *J. Futures Markets*, **38** (2018), 586–606. https://doi.org/10.1002/fut.21901

31. X. J. He, S. Lin, A fractional Black-Scholes model with stochastic volatility and European option pricing, *Expert Syst. Appl.*, **178** (2021), 114983. https://doi.org/10.1016/j.eswa.2021.114983

32. X. J. He, W. T. Chen, Pricing foreign exchange options under a hybrid Heston-Cox-Ingersoll-Ross model with regime switching, *IMA J. Manag. Math.*, **33** (2022), 255–272. https://doi.org/10.1093/imaman/dpab013

33. X. J. He, S. Lin, An analytical approximation formula for barrier option prices under the Heston model, *Comput. Econ.*, 2021. https://doi.org/10.1007/s10614-021-10186-7

34. X. J. He, W. T. Chen, A closed-form pricing formula for European options under a new stochastic volatility model with a stochastic long-term mean, *Math. Financ. Econ.*, **15** (2021), 381–396. https://doi.org/10.1007/s11579-020-00281-y

35. Y. Liu, X. Y. Bai, Investor sentiment, option implied information and prediction of stock market volatility, *Secur. Market. Her.*, **1** (2020), 54–61.

36. X. M. Wang, Empirical analysis of Shanghai 50ETF options pricing based on local volatility model, *Syst. Eng.-Theor. Pract.*, **39** (2019), 2487–2501.

AIMS Press

© 2022 the Author(s), licensee AIMS Press. This is an open access article distributed under the terms of the Creative Commons Attribution License (http://creativecommons.org/licenses/by/4.0)